Velocity and energy distributions in microcanonical ensembles of hard spheres

Enrico Scalas,[1,2,*] Adrian T. Gabriel,[3,†] Edgar Martin,[3,‡] and Guido Germano[3,4,§]

[1] *Department of Sciences and Technological Innovation, Laboratory on Complex Systems, Amedeo Avogadro University of Eastern Piedmont, Viale Teresa Michel 11, 15121 Alessandria, Italy*

[2] *Basque Center for Applied Mathematics, Alameda de Mazarredo 14, 48009 Bilbao, Basque Country, Spain*

[3] *Department of Chemistry and WZMW, Computer Simulation Group, Philipps-University Marburg, 35032 Marburg, Germany*

[4] *Scuola Normale Superiore, Piazza dei Cavalieri 7, 56126 Pisa, Italy*

(Dated: December 7, 2012)

In a microcanonical ensemble (constant NVE, hard reflecting walls) and in a molecular dynamics ensemble (constant $NVE\mathbf{PG}$, periodic boundary conditions) with a number N of hard spheres in a d-dimensional volume V having a total energy E, a total momentum $\mathbf{P}$, and an overall center of mass position $\mathbf{G}$, the individual velocity components, velocity moduli, and energies follow transformed beta distributions with different arguments and shape parameters depending on d, N, E, the boundary conditions, and possible symmetries in the initial conditions. This can be shown marginalizing the joint distribution of individual energies, which is a symmetric Dirichlet distribution. In the thermodynamic limit the beta distributions converge to gamma distributions with different arguments and shape or scale parameters, corresponding respectively to the Gaussian, i.e., Maxwell-Boltzmann, Maxwell, and Boltzmann or Boltzmann-Gibbs distribution. These analytical results are in agreement with molecular dynamics and Monte Carlo simulations with different numbers of hard disks or spheres and hard reflecting walls or periodic boundary conditions.

PACS numbers: 02.50.-r 02.50.Ng, 02.70.Uu, 05.10.-a, 05.10.Ln, 07.05.Tp

I. INTRODUCTION

The problem of the velocity distribution in a gas of hard spheres was discussed in a paper published by Maxwell in 1860 [1]. Maxwell obtained the velocity distribution by assuming independence of the three components of velocity and rotational invariance of the joint distribution. The only distribution satisfying the functional equation

$$\begin{aligned} f_{\mathbf{v}}(x_1, x_2, x_3) &= \Phi(x_1^2 + x_2^2 + x_3^2) \\ &= f_{v_1}(x_1) f_{v_2}(x_2) f_{v_3}(x_3) \end{aligned} \tag{1}$$

has factors of the form

$$f_{v_\alpha}(x) = A \exp(-Bx^2), \tag{2}$$

$\alpha = 1, 2, 3$. This simple heuristic derivation can still be found in modern textbooks in statistical physics or physical chemistry [2], but generalizations of Maxwell's method appeared earlier in the physical literature [3].

In 1867 Maxwell [4] became aware that Eq. (2) should appear as a stationary solution for the dynamics of the gas and introduced a concept that later was called *Stoßzahlansatz* by Boltzmann. It led to a more detailed study of molecular collisions and to kinetic equations whose stationary solutions coincide with Maxwell's original distribution (see Refs. [5–9] for a modern mathematical approach to kinetic equations). This route was followed by Boltzmann, who obtained the velocity distribution in a more general way in a series of papers written between 1868 and 1871 [10–12]. Based on the *Stoßzahlansatz*, Boltzmann could prove that Maxwell's distribution is stationary. These results are summarized in Tolman's book [13] and in the first chapter of ter Haar's book [14].

The two physicists were not working in isolation and were aware of their respective works. In his 1872 paper, Boltzmann often quotes Maxwell [15]. In 1873, Maxwell wrote to his correspondent Tait [16]:

> By the study of Boltzmann I have been unable to understand him. He could not understand me on account of my shortness, and his length was and is an equal stumbling block to me.

More details on the relationship between Maxwell and Boltzmann and on the influence of Maxwell on Boltzmann's thought have been collected by Uffink [17].

Tolman's analysis of classical binary collisions for hard spheres led to rate equations which can be interpreted as transition probabilities for a Markov chain after proper normalization. The interested reader can consult chapter V of Tolman's classic book [13], in particular the discussion around Eq. (45.3) on page 129. The connection with Markov chains was made explicit by Costantini and Garibaldi [18, 19], who used a model due to Brillouin [20]. Before Costantini and Garibaldi, Penrose

*Electronic address: enrico.scalas@unipmn.it; URL: `http://people.unipmn.it/scalas`

†Electronic address: adrian.gabriel@uni-marburg.de

‡Electronic address: edgar.martin@uni-marburg.de

§Electronic address: guido.germano@uni-marburg.de; URL: `www.uni-marburg.de/fb15/ag-germano`

suggested that a Markovian hypothesis could justify the use of standard statistical mechanical tools [21]. According to our interpretation of Penrose, due to the limits in human knowledge naturally leading to coarse graining, systems of many interacting particles effectively behave as Markov chains. Moreover, the possible number of states of such a chain is finite even if very large, therefore only the theory of finite Markov chains is useful. Statistical equilibrium is reached when the system states obey the equilibrium distribution of the finite Markov chain; this equilibrium distribution exists, is unique and coincides with the stationary distribution if the chain is irreducible or ergodic. This point of view is also known as Markovianism. Indeed, in a recent paper on the Ehrenfest urn, we showed that, after appropriate coarse graining, a Markov chain well approximates the behaviour of a realistic model for a fluid [22].

Here we study the velocity distribution in a system of N smooth elastic hard spheres in d dimensions. Even if the evolution of the system is deterministic, we can consider the velocity components of each particle as random variables. We do not consider a finitary [23] version of the model by discretizing velocities, but keep them as real variables. Then a heuristic justification of Eq. (2) can be based on the central limit theorem (CLT). Here is the argument. Following Maxwell's idea, one can consider the velocity components of each particle independent from each other. Further assuming that velocity jumps after collisions are independent and identically distributed random variables, one obtains for the velocity component α of a particle i at time t

$$v_{i\alpha}(t) = v_{i\alpha}(0) + \sum_{j=1}^{n(t)} \Delta v_{i\alpha,j}, \tag{3}$$

where $n(t)$ is the number of collisions for that particle up to time t and $\Delta v_{i\alpha,j}$ is the change in velocity at collision j. If the hypotheses stated above are valid, Eq. (3) defines a continuous-time random walk and the distribution $f_{v_{i\alpha}}(x,t)$ approaches a normal distribution for large t as a consequence of the CLT. Unfortunately this argument is only approximately true in the case of large systems and false for smaller systems.

In Sec. II we obtain the theoretical probability density functions of the individual energies, velocity moduli and velocity components, starting from the fundamental uniform distribution law in phase space. In Sec. III we present the molecular dynamics method used to simulate hard spheres. Interestingly, the same distributions can be reproduced by a simple Monte Carlo stochastic model introduced in Sec. IV. The numerical results are presented in Sec. V together with some statistical goodness-of-fit tests. Indeed, it turns out that an equilibrium distribution of the velocity components seems to be reached already for $N = 2$ particles and without using any coarse graining. When N grows the equilibrium distribution approaches the normal distribution, Eq. (2). A discussion and a summary follow in Sec. VI.

II. THEORY

We consider a fluid of N hard spheres in d dimensions with the same diameter σ and mass m in a cuboidal box with sides L_α, $\alpha = 1, \ldots, d$. The positions $\mathbf{r}_i$, $i = 1, \ldots, N$ are confined to a d-dimensional box with volume $V = \prod_{\alpha=1}^{d} L_\alpha$, i.e., each position component $r_{i\alpha}$ can vary in the interval $[-L_\alpha/2, L_\alpha/2]$. Elastic collisions transfer kinetic energy between the particles, while the total energy of the system,

$$E = \frac{1}{2}\sum_{i=1}^{N} m_i \mathbf{v}_i \cdot \mathbf{v}_i = \frac{1}{2} m\, \mathbf{v} \cdot \mathbf{v}, \tag{4}$$

does not change in time, i.e., it is a constant of the motion. Therefore, the velocities $\mathbf{v}_i$ are confined to the surface of a hypersphere given by the constraint that the total energy is E, i.e., each velocity component $v_{i\alpha}$ can vary in the interval $[-\sqrt{2E/m}, \sqrt{2E/m}]$ with the restriction on the sum of the squares given by Eq. (4). In other words, the rescaled positions $\mathbf{q}$ with $q_{i\alpha} = r_{i\alpha}/L_\alpha$ are confined to the unit hypercube in dN dimensions, while the rescaled velocity components $\mathbf{u} = \sqrt{m/(2E)}\,\mathbf{v}$ are confined to the surface of the unit hypersphere in dN dimensions defined by the constraint $\mathbf{u} \cdot \mathbf{u} = 1$.

The state of the system is specified by the phase space vector of all velocities and positions $\mathbf{\Gamma} = (\mathbf{v}, \mathbf{r})$, i.e., by $2dN$ variables: the velocity components $v_{i\alpha}$ and the position components $r_{i\alpha}$. However, these variables are not independent because of constraints. For spheres with random velocities and positions confined in a container with hard reflecting walls, the total energy E is conserved (microcanonical ensemble, constant NVE) and thus the number of independent variables is $g = 2dN - 1$. With periodic boundary conditions also the total linear momentum

$$\mathbf{P} = \sum_{i=1}^{N} m_i \mathbf{v}_i = m \sum_{i=1}^{N} \mathbf{v}_i \tag{5}$$

and center of mass

$$\mathbf{G} = \frac{\sum_{i=1}^{N} m_i \mathbf{r}_i}{\sum_{i=1}^{N} m_i} = \frac{1}{N}\sum_{i=1}^{N} \mathbf{r}_i \tag{6}$$

are conserved (molecular dynamics ensemble, constant $NVE\mathbf{PG}$), and thus the number of independent variables drops to $g = 2d(N-1) - 1 = 2dN - 2d - 1$. Symmetries in the positions and velocities may reduce g too; e.g. if all components i of $\mathbf{\Gamma}$ are pairwise symmetric with respect to the origin, with both kinds of boundary conditions this point symmetry will stay on forever and $g = dN - 1$ or $g = 2d(N/2 - 1) - 1 = dN - 2d - 1$ respectively. For the sake of simplicity, in presenting the theory we will treat explicitly only the microcanonical case without symmetries.

Following Khinchin, one can assume the uniform distribution in the accessible portion of phase space as the

starting point of statistical mechanics [24]. In our case, the measure of the accessible region of phase space is the product of the volume of the dN-dimensional hypercube times the surface of the dN-dimensional hypersphere,

$$\Omega = V^N \frac{2\pi^{dN/2}}{\Gamma(dN/2)} \left(\frac{2E}{m}\right)^{(dN-1)/2}. \quad (7)$$

This applies to a phase space whose coordinates are velocities and positions; of course the expression will be slightly different using momenta rather than velocities, or if the so-called density of states with respect to the energy, $\Omega' = \mathrm{d}\Omega/\mathrm{d}E$, is used instead [24].

Khinchin's *Ansatz* is that the probability density function (PDF) for points $(\mathbf{v}, \mathbf{r})$ in the permitted region of phase space is uniform. However, so far this has not been rigorously proved in general. In our case this *Ansatz* leads to the joint PDF for velocities and positions

$$f_{\mathbf{v},\mathbf{r}}(\mathbf{x},\mathbf{y}) = \frac{1}{\Omega}\mathbf{1}_{\left\{\mathbf{x}\cdot\mathbf{x}=\frac{2E}{m}\right\}}(\mathbf{x})\mathbf{1}_{\prod_{\alpha=1}^{d}\left[-\frac{L_\alpha}{2},\frac{L_\alpha}{2}\right]^N}(\mathbf{y}), \quad (8)$$

where $\mathbf{1}_A(\mathbf{x})$ is the indicator function of the set A,

$$\mathbf{1}_A(\mathbf{x}) \stackrel{\text{def}}{=} \begin{cases} 1 & \text{if } \mathbf{x} \in A \\ 0 & \text{if } \mathbf{x} \notin A \end{cases}. \quad (9)$$

As the energy does not depend on positions, one can integrate over the latter, yielding a uniform PDF for particle velocities on the surface of a hypersphere,

$$f_{\mathbf{v}}(\mathbf{x}) = \frac{\Gamma(dN/2)}{2\pi^{dN/2}} \left(\frac{m}{2E}\right)^{(dN-1)/2} \mathbf{1}_{\left\{\mathbf{x}\cdot\mathbf{x}=\frac{2E}{m}\right\}}(\mathbf{x}). \quad (10)$$

The marginalization of this joint PDF leads to the distributions of individual particle energies as well as of velocity moduli and velocity components. To this purpose, it is convenient to study the relationship between Eq. (10) and the symmetric Dirichlet distribution with parameter a.

The PDF of the n-dimensional Dirichlet distribution with parameter vector $\mathbf{a}$ is

$$f^{\mathrm{D}}_{\mathbf{X}}(\mathbf{x};\mathbf{a}) \stackrel{\text{def}}{=} \frac{1}{\mathrm{B}(\mathbf{a})} \prod_{i=1}^{n} x_i^{a_i-1} \prod_{i=1}^{n} \mathbf{1}_{[0,1]}(x_i)\mathbf{1}_{\left\{\sum_{i=1}^n x_i = 1\right\}}(\mathbf{x}). \quad (11)$$

Its value is zero outside the unit simplex

$$S = \left\{ \mathbf{x} \in \mathbb{R}^n : \forall i \; x_i \geq 0 \wedge \sum_{i=1}^{n} x_i = 1 \right\}, \quad (12)$$

and thus Eq. (11) can also be written

$$f^{\mathrm{D}}_{\mathbf{X}}(\mathbf{x};\mathbf{a}) \stackrel{\text{def}}{=} \frac{1}{\mathrm{B}(\mathbf{a})} \prod_{i=1}^{n} x_i^{a_i-1} \mathbf{1}_S(\mathbf{x}). \quad (13)$$

The normalization factor is given by the multinomial beta function, which can be defined through the gamma function,

$$\mathrm{B}(\mathbf{a}) = \frac{\prod_{i=1}^{n}\Gamma(a_i)}{\Gamma(\sum_{i=1}^{n} a_i)}. \quad (14)$$

The multinomial beta function is a generalization of the beta function or Euler integral of the first kind, $\mathrm{B}(x,y) = \int_0^1 t^{x-1}(1-t)^{y-1}\mathrm{d}t$, which can be expressed through the gamma function or Euler integral of the second kind, $\Gamma(z) = \int_0^\infty e^{-t}t^{z-1}\mathrm{d}t$, as $\mathrm{B}(x,y) = \Gamma(x)\Gamma(y)/\Gamma(x+y)$. In the symmetric Dirichlet distribution all elements of the parameter vector $\mathbf{a}$ have the same value $a_i = a$,

$$f^{\mathrm{D}}_{\mathbf{X}}(\mathbf{x};a) \stackrel{\text{def}}{=} \frac{\Gamma(na)}{[\Gamma(a)]^n} \prod_{i=1}^{n} x_i^{a-1} \mathbf{1}_S(\mathbf{x}). \quad (15)$$

Notice that $a = 1$ gives the uniform distribution on S.

It is convenient to work with dimensionless variables. With the rescaling $u_{i\alpha} = \sqrt{m/(2E)}\, v_{i\alpha}$ introduced above, one gets the PDF

$$f_{\mathbf{u}}(\mathbf{x}) = \frac{\Gamma(dN/2)}{2\pi^{dN/2}} \mathbf{1}_{\{\mathbf{x}\cdot\mathbf{x}=1\}}(\mathbf{x}). \quad (16)$$

A second transformation

$$w_{i\alpha} = u_{i\alpha}^2 \quad (17)$$

leads to a set of dN random variables each one with support in [0,1] and such that

$$\sum_{i=1}^{N}\sum_{\alpha=1}^{d} w_{i\alpha} = 1. \quad (18)$$

The Jacobian for this transformation is

$$\left|\frac{\partial \mathbf{u}}{\partial \mathbf{w}}\right| = \frac{1}{2^{dN}} \prod_{i=1}^{N}\prod_{\alpha=1}^{d} w_{i\alpha}^{-1/2}. \quad (19)$$

Multiplying it by a factor 2^{dN} because each $\pm u_{i\alpha}$ results in the same $w_{i\alpha}$ and by another factor 2 because of the constraint given by Eq. (18) (for details see Song and Gupta [25]), and replacing $\sqrt{\pi} = \Gamma(1/2)$, the joint PDF of the variables $w_{i\alpha}$ can be expressed through the symmetric Dirichlet PDF with parameter $a = 1/2$,

$$\begin{aligned} f_{\mathbf{w}}(\mathbf{x}) &= f^{\mathrm{D}}_{\mathbf{w}}(\mathbf{x};1/2) \\ &= \frac{\Gamma(dN/2)}{[\Gamma(1/2)]^{dN}} \prod_{i=1}^{N}\prod_{\alpha=1}^{d} x_{i\alpha}^{-1/2} \mathbf{1}_S(\mathbf{x}). \end{aligned} \quad (20)$$

Now the normalized energy per particle,

$$\varepsilon_i = \frac{E_i}{E} = \frac{mv_i^2}{2E} = \sum_{\alpha=1}^{d} w_{i\alpha}, \quad (21)$$

is the sum of d variables following the distribution given by Eq. (20). As a consequence of the aggregation law for

Dirichlet distributions, one finds that the joint PDF of all ε_i is

$$\begin{aligned} f_{\boldsymbol{\varepsilon}}(\mathbf{x}) &= f^{\mathrm{D}}_{\boldsymbol{\epsilon}}(\mathbf{x}; d/2) \\ &= \frac{\Gamma(dN/2)}{[\Gamma(d/2)]^N} \prod_{i=1}^{N} x_i^{d/2-1} \mathbf{1}_S(\mathbf{x}). \end{aligned} \tag{22}$$

It is interesting to notice that this is a uniform distribution for $d = 2$; because of this, Boltzmann's 1868 method works in $d = 2$ dimensions, but fails in $d = 3$ dimensions [10].

The PDF of the normalized energies of single particles can be obtained by a further marginalization of the symmetric Dirichlet distribution given by Eq. (22), using again the aggregation law. The result is a beta distribution, whose PDF is

$$f^{\beta}_X(x; a, b) \stackrel{\text{def}}{=} \frac{1}{\mathrm{B}(a,b)} x^{a-1}(1-x)^{b-1} \mathbf{1}_{[0,1]}(x), \tag{23}$$

i.e. a Dirichlet distribution, Eq. (11), with $n = 2$. In other words, the Dirichlet distribution is a multivariate generalization of the beta distribution. Our case has the exponents $a = d/2$ and $b = d(N-1)/2$,

$$\begin{aligned} f_{\varepsilon_i}(x) &= f^{\beta}_{\varepsilon_i}\left(x; \frac{d}{2}, \frac{d(N-1)}{2}\right) \\ &= \frac{\Gamma(dN/2)}{\Gamma(d/2)\Gamma(d(N-1)/2)} x^{d/2-1} \\ &\quad \times (1-x)^{d(N-1)/2-1} \mathbf{1}_{[0,1]}(x). \end{aligned} \tag{24}$$

The transformation of variables $E_i = E\varepsilon_i$ immediately leads to the PDF of particle energies, that follow a beta-Stacy distribution,

$$\begin{aligned} f_{E_i}(x) &= f^{\beta}_{E_i}\left(\frac{x}{E}; \frac{d}{2}, \frac{d(N-1)}{2}\right) \frac{\mathrm{d}}{\mathrm{d}x}\frac{x}{E} \\ &= \frac{\Gamma(dN/2)}{\Gamma(d/2)\Gamma(d(N-1)/2)} \left(\frac{x}{E}\right)^{d/2} \\ &\quad \times \left(1 - \frac{x}{E}\right)^{d(N-1)/2-1} \frac{1}{E} \mathbf{1}_{[0,E]}(x) \end{aligned} \tag{25}$$

for $N > 1$, and $f_{E_i}(x) = \delta(x - E)$ for $N = 1$. This result was obtained with a different method, without invoking the Dirichlet and beta distributions, by Shirts et al. [26, Eq. (9)].

In the thermodynamic limit ($N, V, E \to \infty$ with $N/V = \rho =$ constant and $E/N = \bar{E} =$ constant), Eq. (25) converges to a gamma distribution, as discussed by Garibaldi and Scalas [23, pages 121–122]. The gamma PDF is

$$f^{\gamma}_X(x; a, b) \stackrel{\text{def}}{=} \frac{x^{a-1}}{b^a \Gamma(a)} \exp\left(-\frac{x}{b}\right) \mathbf{1}_{[0,\infty)}(x). \tag{26}$$

A scale parameter is usually included in the definition of the gamma distribution, but it could always be set to 1 absorbing it into the argument,

$$f^{\gamma}_X(x; a, b) = f^{\gamma}_X\left(\frac{x}{b}; a, 1\right) \frac{1}{b} \equiv f^{\gamma}_X\left(\frac{x}{b}; a\right) \frac{1}{b}. \tag{27}$$

Coming back to the thermodynamic limit of Eq. (25) anticipated above, this is a gamma distribution with shape parameter $a = d/2$ and scale parameter $b = 2\bar{E}/(dm)$,

$$\begin{aligned} f_{E_i}(x) &= f^{\gamma}_{E_i}\left(x; \frac{d}{2}, \frac{2\bar{E}}{dm}\right) \\ &= \left(\frac{dm}{2\bar{E}}\right)^{d/2} \frac{x^{d/2-1}}{\Gamma(d/2)} \exp\left(-\frac{dmx}{2\bar{E}}\right) \mathbf{1}_{[0,\infty)}(x), \end{aligned} \tag{28}$$

which is the familiar Boltzmann or Boltzmann-Gibbs distribution for $d = 2$.

The PDF of the velocity moduli, or speeds, of individual particles can be obtained from $f_{E_i}(x)$ replacing $v_i = \sqrt{2E_i/m}$. The result is a transformed beta-Stacy distribution with the same exponents $a = d/2$ and $b = d(N-1)/2$ as for the energies, but argument $mx^2/(2E)$,

$$\begin{aligned} f_{v_i}(x) &= f^{\beta}_{v_i}\left(\frac{mx^2}{2E}; \frac{d}{2}, \frac{d(N-1)}{2}\right) \frac{\mathrm{d}}{\mathrm{d}x}\frac{mx^2}{2E}, \\ &= \frac{\Gamma(dN/2)}{\Gamma(d/2)\Gamma(d(N-1)/2)} \left(\frac{mx^2}{2E}\right)^{\frac{d}{2}-1} \\ &\quad \times \left(1 - \frac{mx^2}{2E}\right)^{\frac{d(N-1)}{2}-1} \frac{mx}{E} \mathbf{1}_{\left[0, \sqrt{\frac{2E}{m}}\right]}(x) \end{aligned} \tag{29}$$

for $N > 1$, and $f_{v_i}(x) = \delta(x - \sqrt{2E/m})$ for $N = 1$. Also this result was obtained with a different method by Shirts et al. [26].

In the thermodynamic limit, Eq. (29) converges to the transformed gamma distribution with argument $x^2/2$, shape parameter $a = d/2$ and scale parameter $b = 2\bar{E}/(dm)$,

$$\begin{aligned} f_{v_i}(x) &= f^{\gamma}_{v_i}\left(\frac{x^2}{2}; \frac{d}{2}, \frac{2\bar{E}}{dm}\right) \frac{\mathrm{d}}{\mathrm{d}x}\frac{x^2}{2} \\ &= \left(\frac{dm}{\bar{E}}\right)^{\frac{d}{2}} \frac{(x/2)^{d-1}}{\Gamma(d/2)} \exp\left(-\frac{dmx^2}{4\bar{E}}\right) \mathbf{1}_{[0,\infty)}(x) \end{aligned} \tag{30}$$

which is the familiar Maxwell distribution for $d = 3$.

The transformation from hyperspherical coordinates to cartesian coordinates $v_i^2 = \sum_{\alpha=1}^{d} v_{i\alpha}^2$ and $(2\pi^{d/2}/\Gamma(d/2)) v_i^{d-1} \mathrm{d}v_i = \prod_{\alpha=1}^{d} \mathrm{d}v_{i\alpha}$ leads from Eq. (29) to the PDF $f_{\mathbf{v}_i}(\mathbf{x})$ of the single-particle velocity vectors

$$\begin{aligned} f_{\mathbf{v}_i}(\mathbf{x}) &= \frac{\Gamma(dN/2)}{\Gamma(d(N-1)/2)} \left(\frac{m}{2\pi E}\right)^{d/2} \\ &\quad \times \left(1 - \frac{m}{2E}\mathbf{x}\cdot\mathbf{x}\right)^{d(N-1)/2-1} \mathbf{1}_{\left\{\mathbf{x}\cdot\mathbf{x} = \frac{2E}{m}\right\}}(\mathbf{x}), \end{aligned} \tag{31}$$

an equation obtained before too [26, 27].

The direct marginalization [25] of the joint PDF of all velocities, Eq. (10), leads to the PDF $f_{v_{i\alpha}}(x)$ of velocity components, a result obtained integrating over all i except one and over all α except one. This is the quantity discussed by Maxwell [1], and its derivation for any

N is one of the main results in this paper. It turns out that the PDF of the velocity components is a transformed beta distribution with argument $\left(1+\sqrt{m/(2E)}\,x\right)/2$ and equal exponents $a=b=(dN-1)/2$,

$$\begin{aligned} f_{v_{i\alpha}}(x) &= \frac{1}{2}\sqrt{\frac{m}{2E}}\frac{\mathbf{1}_{\left[-\sqrt{\frac{2E}{m}},\sqrt{\frac{2E}{m}}\right]}(x)}{\mathrm{B}((dN-1)/2,(dN-1)/2)} \\ &\quad\times\left[\left(\frac{1}{2}+\sqrt{\frac{m}{2E}}\frac{x}{2}\right)\left(\frac{1}{2}-\sqrt{\frac{m}{2E}}\frac{x}{2}\right)\right]^{(dN-3)/2} \\ &= \frac{1}{2^{dN-2}}\sqrt{\frac{m}{2E}}\frac{\Gamma(dN-1)}{\Gamma^2((dN-1)/2)} \\ &\quad\times\left(1-\frac{mx^2}{2E}\right)^{(dN-3)/2}\mathbf{1}_{\left[-\sqrt{\frac{2E}{m}},\sqrt{\frac{2E}{m}}\right]}(x) \\ &= f^{\beta}_{v_{i\alpha}}\left(\frac{1}{2}+\sqrt{\frac{m}{2E}}\frac{x}{2};\frac{dN-1}{2},\frac{dN-1}{2}\right) \\ &\quad\times\frac{\mathrm{d}}{\mathrm{d}x}\left(\frac{1}{2}+\sqrt{\frac{m}{2E}}\frac{x}{2}\right). \end{aligned} \tag{32}$$

In the thermodynamic limit Eq. (32) converges to a normal law with average $\mu=0$ and variance $\sigma^2=d\bar{E}/(2m)$, i.e. the familiar Maxwell-Boltzmann distribution

$$f_{v_{i\alpha}}(x)=\sqrt{\frac{m}{d\pi\bar{E}}}\exp\left(-\frac{mx^2}{d\bar{E}}\right). \tag{33}$$

This is again related to a gamma distribution, since the positive half of the normal distribution can be expressed as

$$\frac{2}{\sqrt{2\pi}\sigma}\exp\left(-\frac{x^2}{2\sigma^2}\right)\mathbf{1}_{[0,\infty)}(x)=f^{\gamma}_{X}\left(\frac{x^2}{2};\frac{1}{2},\sigma^2\right)\frac{\mathrm{d}}{\mathrm{d}x}\frac{x^2}{2}. \tag{34}$$

In summary, all the known results for the relevant distributions of the NVE ensemble can be obtained observing that the normalized individual particle energies $\varepsilon_i=E_i/E$ follow a symmetric multivariate Dirichlet distribution with parameter $a=1/2$ given by Eq. (20). This is a direct consequence of the uniform-distribution assumption in Eq. (8) via a simple change of variables. Only for the velocity components it is necessary to marginalize the uniform distribution directly on the surface of the hypersphere and not on the simplex. Maxwell's *Ansatz* is vindicated by the fact that, in the thermodynamic limit, a normal distribution for velocity components is recovered, as well as their independence. Finally, for the $NVE\mathbf{PG}$ ensemble, the constraint given in Eq. (5) leads to different distributions for the relevant quantities introduced above. This will become clearer in the following.

III. MOLECULAR DYNAMICS SIMULATIONS

In molecular dynamics (MD) with continuous potentials, the equations of motion are integrated numerically using a constant time step; this approach is called time-driven. The larger the forces, the smaller the time step necessary to ensure energy conservation. With step potentials there are no forces acting on a distance, only impulsive ones at the exact time of impact. Therefore an event-driven approach is more appropriate: rather than until a fixed time step, the system is propagated until either the next collision or the next boundary crossing [28–31].

The collision time t_{ij} between two particles i,j can be calculated from the mutual distance $\mathbf{r}_{ij}=\mathbf{r}_i-\mathbf{r}_j$ and the relative velocity $\mathbf{v}_{ij}=\mathbf{v}_i-\mathbf{v}_j$. If $b_{ij}=\mathbf{v}_{ij}\cdot\mathbf{r}_{ij}>0$ the particles are moving away from each other and will not collide. Otherwise impact may happen at time t_{ij} when their distance becomes equal to the sum of their radii, i.e., $\|\mathbf{r}_{ij}+t_{ij}\mathbf{v}_{ij}\|=\sigma$. This is a second order problem with solutions

$$t^{\pm}_{ij}=\frac{-b_{ij}\pm\sqrt{b_{ij}^2-v_{ij}^2(r_{ij}^2-\sigma^2)}}{v_{ij}^2}. \tag{35}$$

If the solutions are complex, no collision occurs. If the solutions are real, the smaller one, t^{-}_{ij}, corresponds to when the particles first meet, while the larger one, t^{+}_{ij}, to when they leave each other assuming they are allowed to interpenetrate. A negative collision time means that the event took place in the past. Because of the condition $b_{ij}<0$, at least $t^{+}_{ij}>0$. If $t^{-}_{ij}<0$ the particles overlap, which indicates an error. So the collision time is given by t^{-}_{ij}, provided it is a positive real number.

For a system of N hard spheres, at impact, assuming an elastic collision, the total kinetic energy E and the total linear momentum $\mathbf{P}$ are conserved (usually one sets $\mathbf{P}=\mathbf{0}$ at the beginning of the simulation by subtracting $\frac{1}{N}\sum_{i=1}^{N}\mathbf{v}_i$ from each $\mathbf{v}_i$). Assuming smooth surfaces, the impulse acts along the line of centers of the collision partners i and j given by $\hat{\mathbf{r}}_{ij}$; with equal masses, $\mathbf{v}_i$ changes to $\mathbf{v}_i+\Delta\mathbf{v}_i$ and $\mathbf{v}_j$ changes to $\mathbf{v}_j-\Delta\mathbf{v}_i$ with

$$\Delta\mathbf{v}_i=-\frac{b_{ij}\mathbf{r}_{ij}}{\sigma^2}=-(\mathbf{v}_{ij}\cdot\hat{\mathbf{r}}_{ij})\,\hat{\mathbf{r}}_{ij}=-\mathbf{v}^{\parallel}_{ij}, \tag{36}$$

where $\mathbf{r}_{ij}$ and $\mathbf{v}_{ij}$ are evaluated at the instant of collision, and thus $\|\mathbf{r}_{ij}\|=\sigma$.

When a particle reaches a side of the unit box, periodic boundary conditions may require to "rebox" it by reintroducing it on the other side, while hard reflecting walls require to invert the velocity component perpendicular to the wall. After an event, be it a collision with another particle, a boundary crossing or a reflection at a boundary, the event calendar must be re-evaluated for pairs involving one of the event participants or a particle scheduled to collide with one of the event participants. All other particles are not influenced. Thus not every scheduled event actually takes place, because it can be invalidated by another earlier event, in which case it is erased from the priority queue. The latter is most commonly handled by means of a binary tree [32], which we realized with a multimap of the C++ Standard Template Library [33]. The efficiency of this and alternative data

structures for event scheduling has been analyzed extensively [34, 35].

The computational effort to search for $\min_{i,j} t_{ij}$ grows as the square of the number of particles; see Fig. 1 (top). For large systems it is advisable to divide the simulation box into cells [36], which makes the dependence of the CPU time on the number of particles linear; see Fig. 1 (bottom). Provided cell boundary crossings are considered too in the event list, two particles can collide only if they are located in the same cell or in adjacent cells. We chose cells with a side larger than a particle diameter. For more details on this and other algorithmic aspects in event-driven MD see Refs. [37–39]. For a parallel implementation see Miller and Luding [40].

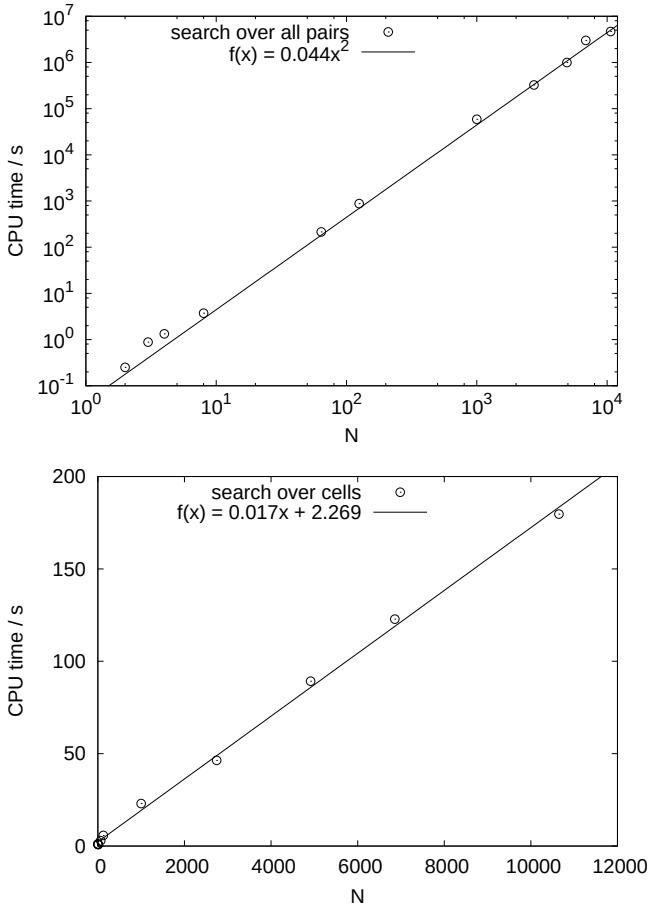

FIG. 1: CPU time for 10^5 collisions on a 2.2 GHz AMD Athlon 64 X2 "Toledo" as a function of the number of hard spheres N for our event-based MD programs with a simple search over all pairs (top) and an optimized search over cells (bottom). The data are fitted respectively with a quadratic and a linear function, which cross-over between $N = 3$ and $N = 4$.

IV. MONTE CARLO SIMULATIONS

Except for especially ordered initial conditions, interparticle collisions computed by MD as explained in Sec. III have mutual distance versors at collision $\hat{\mathbf{r}}_{ij}$ uniformly distributed on a unit half sphere in d dimensions such that, given relative velocities $\mathbf{v}_{ij}$, the scalar product $\mathbf{v}_{ij} \cdot \hat{\mathbf{r}}_{ij}$ is negative. Therefore the same distributions of velocities, and thus of derived quantities like energies, as in MD with periodic boundaries can be obtained by Monte Carlo (MC): after initializing the velocities of all hard spheres, the MC cycles consist in selecting a pair ij and a random versor $\hat{\mathbf{r}}_{ij}$ such that $\mathbf{v}_{ij} \cdot \hat{\mathbf{r}}_{ij} < 0$, and then in updating the velocities according to Eq. (36). Hard reflecting walls can be included in the MC scheme by selecting with a certain frequency a sphere i and inverting one of its velocity components $v_{i\alpha}$. This scheme gives a useful insight into the mechanism of energy and momentum transfer. It is much easier to code and faster to run than MD, especially for large numbers of particles N, because no event list management is necessary: on the same computer used for the MD benchmarks shown in Fig. 1, 10^5 MC collisions with $N = 10\,000$ spheres take a CPU time of 0.3 s.

For a given initial state, i.e. a set of particle velocities, the MC dynamics defined above provides the realization of a Markov chain with a symmetric transition kernel, meaning that $P(\mathbf{v}'|\mathbf{v}) = P(\mathbf{v}|\mathbf{v}')$, where $\mathbf{v}$ is the old velocity vector before the transition and $\mathbf{v}'$ is the new velocity vector after the transition. This Markov chain is homogeneous, as the transition probability does not depend on the time step. Invoking detailed balance, $P(\mathbf{v}'|\mathbf{v})P(\mathbf{v}) = P(\mathbf{v}|\mathbf{v}')P(\mathbf{v}')$, the symmetry of the transition kernel implies that the stationary distribution of this chain is uniform over the set of accessible states. If this set coincides with the surface of the velocity hypersphere, then the Markov chain is ergodic and one can hope to prove that the uniform distribution over the hypershere is also the equilibrium distribution for the Markov chain; see Sigurgeirsson [41, Chapter 5] for the discussion of a related problem, and Meyn and Tweedie [42] for general methods. The results of MC simulations described below corroborate this conjecture and the algorithm outlined above is indeed an effective way of sampling the uniform distribution on the surface of a hypersphere.

V. NUMERICAL RESULTS

Probability density functions $f_{v_{i\alpha}}$ of the velocity components, f_{v_i} of the velocity modulus, and f_{E_i} of the energy for $N = 2$, 3, 4, 10, 100, 1000 hard disks ($d = 2$) and hard spheres ($d = 3$) from theory (Sec. II) as well as from MD (Sec. III) and MC simulations (Sec. IV) are shown in Fig. 2 for a microcanonical ensemble (constant NVE, hard reflecting walls) and in Fig. 3 for a molecular dynamics ensemble (constant NVE**PG**, periodic boundary conditions). In reduced units [30] the particle mass is $m = 1$, the particle diameter is $\sigma = 1$, the energy per particle is $\bar{E} = 1$, the Boltzmann constant is $k_B = 1$, the number density is $\rho = 2/3^d$, the initial total mo-

mentum is $\mathbf{P} = \mathbf{0}$, and the initial position of the center of mass is $\mathbf{G} = \mathbf{0}$. The density appears only in MD, and the results are largely independent of this parameter, as long as it is not too large (in this case the particles cannot move freely) or too small (in this case the particles hardly ever collide). The numerical simulations were equilibrated over 5×10^5 collisions and sampled over 10^6 collisions. The agreement between theory, MD and MC is excellent, with little systematic deviations only for MD with the smallest values of N. Unfortunately so far the reason for these deviations could not be found.

The PDF $f_{v_{i\alpha}}(x)$ for $d = 2$ and $N = 2$ in the $NVE\mathbf{PG}$ ensemble is the arcsine law,

$$f_{v_{i\alpha}}(x) = \frac{1}{\pi\sqrt{2\bar{E}/m - x^2}}, \tag{37}$$

which is bimodal. The name is due to its cumulative distribution function,

$$F_{v_{i\alpha}}(x) = \frac{1}{\pi} \arcsin\left(\sqrt{\frac{m}{2\bar{E}}}x\right) + \frac{1}{2}. \tag{38}$$

For $d = 2$ and $N = 2$ in the NVE ensemble and for $d = 2$ and $N = 3$ in the $NVE\mathbf{PG}$ ensemble, $f_{v_{i\alpha}}(x)$ is the semicircle law,

$$f_{v_{i\alpha}}(x) = \frac{m}{2\pi\bar{E}}\sqrt{\frac{4\bar{E}}{m} - x^2}. \tag{39}$$

Its cumulative distribution function again contains an arcsine,

$$F_{v_{i\alpha}}(x) = \frac{mx}{4\pi\bar{E}}\sqrt{\frac{m}{4\bar{E}} - x^2} + \frac{1}{\pi} \arcsin\left(\sqrt{\frac{m}{4\bar{E}}}x\right) + \frac{1}{2}. \tag{40}$$

For the same systems, f_{E_i} is a uniform distribution on $[0, 2]$.

For $d = 3$ and $N = 2$ in the $NVE\mathbf{PG}$ ensemble, $f_{v_{i\alpha}}(x)$ is a uniform distribution on $[-\sqrt{2}, \sqrt{2}]$.

All these distributions are given by Eqs. (25), (29) and (32) inserting the appropriate values of d, N and E for the NVE ensemble, while for the $NVE\mathbf{PG}$ N has to be substituted by $N - 1$ because of the additional constraint on the linear momentum. To quantify the visual impression, we performed a Kolmogorov-Smirnov (KS) goodness-of-fit test [43–45] comparing Eq. (32) with the empirical cumulative distribution function of MC velocity components for $d = 2$ in the $NVE\mathbf{PG}$ ensemble for a few selected values of N; see Tab. I. In all cases the null hypothesis of data distributed according to the model equation cannot be rejected at the 5% significance level.

The empirical density $f_{v_{i\alpha}}$ is well approximated by a normal law already for $N = 1000$ hard disks, as shown in Tab. II, where the results of two non-parametric tests for normality, Lilliefors [46] and Jarque and Bera [47, 48], are presented when $N = 10, 100, 1000, 10\,000$; again these tests are done only for MC velocities.

N	Kolmogorov-Smirnov	p_{KS}
2	4.1×10^{-4}	0.99
3	1.0×10^{-3}	0.24
10	1.3×10^{-3}	0.07
100	7.1×10^{-4}	0.69
1000	6.2×10^{-4}	0.84
10 000	1.1×10^{-3}	0.15

TABLE I: Comparison between the empirical probability density functions of the velocity components from MC with periodic boundary conditions and $d = 2$ by means of the KS test. In each case the sample size is 2×10^6. At the 5% significance level the critical value is 9.6×10^{-4}. The null hypothesis of equally distributed data can never be rejected.

N	Lilliefors	p_{L}	Jarque-Bera	p_{JB}
10	0.008*	$< 10^{-3}$	7.4×10^{3}*	$< 10^{-3}$
100	7.36×10^{-4}*	0.01	29.6*	$< 10^{-3}$
1000	4.79×10^{-4}	0.35	5.70	0.06
10 000	4.37×10^{-4}	0.50	2.36	0.31

TABLE II: Results of two non-parametric normality tests for the empirical probability density function of the velocity components from MC with periodic boundary conditions when $d = 2$: Lilliefors (L) and Jarque and Bera (JB). In each case the sample size is 2×10^6. At the 5% significance level the critical value is 6.43×10^{-4} for the L test and 5.99 for the JB test. The star indicates that the null hypothesis of normally distributed data can be rejected.

VI. DISCUSSION AND CONCLUSIONS

To summarize what we have done, in a system of N hard balls in a d-dimensional volume V the velocity components, the velocity modulus and the energies of the spheres or disks are well reproduced by transformed beta distributions with different arguments and shape parameters depending on N, d, the total energy E, and the boundary conditions; in the thermodynamic limit these distributions converge to transformed gamma distributions with different arguments and shape or scale parameters, corresponding respectively to the Gaussian, i.e. Maxwell-Boltzmann, the Maxwell, and the Boltzmann or Boltzmann-Gibbs distribution. We showed this theoretically using Khinchin's *Ansatz*, and performed statistical goodness-of-fit tests on systematic MD and MC computer simulations of an increasing number N of hard disks or spheres starting from 2 in the microcanonical ensemble (constant NVE, hard reflecting walls) and in the molecular dynamics ensemble (constant $NVE\mathbf{PG}$, periodic boundary conditions). The MC simulations are a simple stochastic model based on a generalization of Eq. (3) able to reproduce the same empirical equilibrium distribution for the random variables $v_{i\alpha}$, v_i and E_i as obtained deterministically with canonic dynamics by MD simulations. Even if these results are not entirely new, we presented comprehensively both the analytical

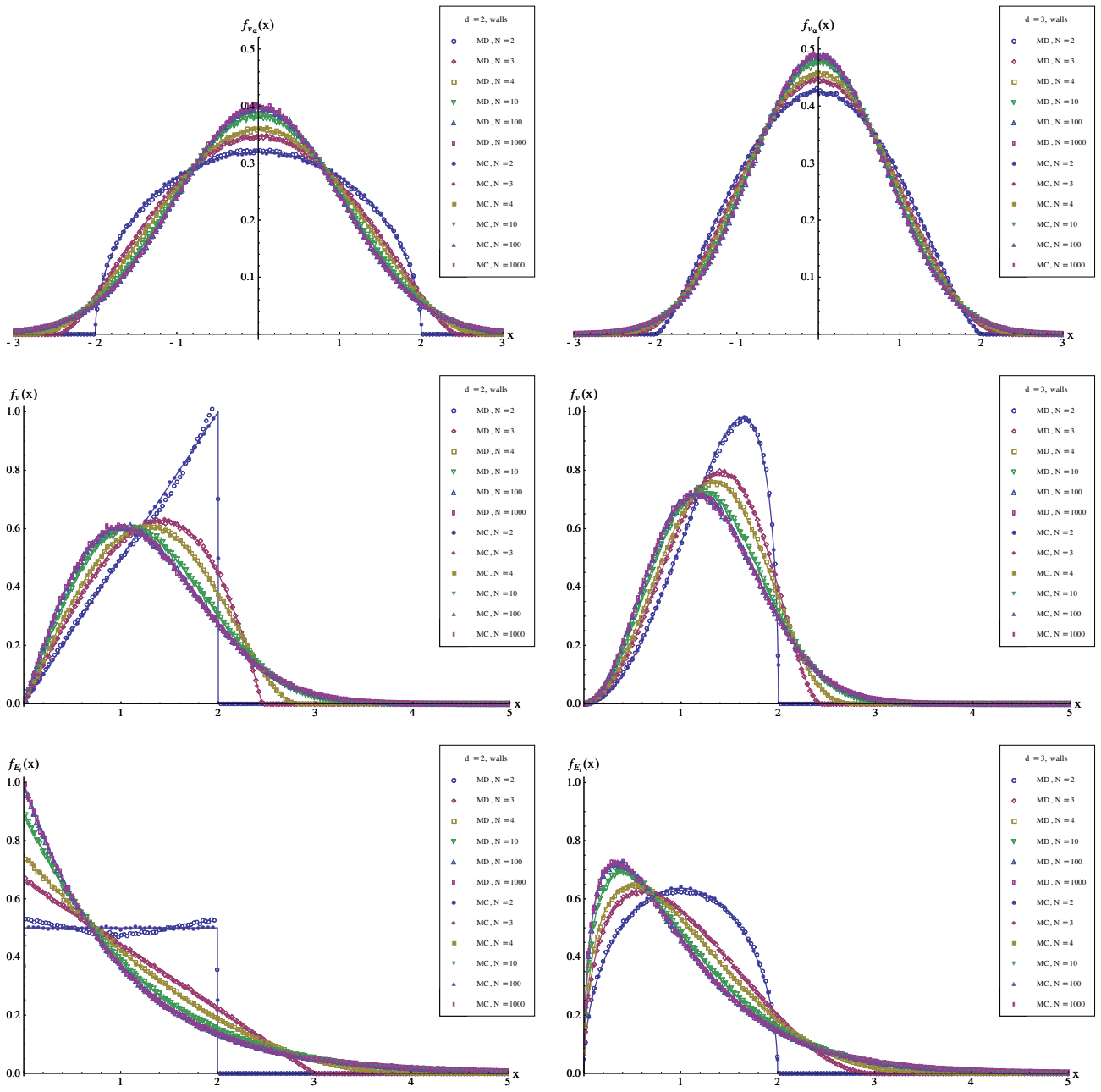

FIG. 2: (Color online) Probability density functions $f_{v_{i\alpha}}$ of the velocity components (top), f_{v_i} of the velocity modulus (middle), and f_{E_i} of the energy (bottom) for $d = 2$ (left) and $d = 3$ (right) with $\bar{E} = 1$ in the microcanonical ensemble (constant NVE, hard reflecting walls): theory (lines), MD (empty symbols), and MC (full symbols). Delta functions are made visible by a vertical line for the theory and by rescaling down to 1 the data point that would otherwise be out of scale.

derivations and the numerical checks, the latter both by MD and MC; moreover, we realized that all these distributions are actually variants of the beta or the gamma distribution, and can be derived from the Dirichlet distribution; and we pointed out that for values of N as low as 2 or 3 the shapes of these distributions can be quite different from those in the thermodynamic limit: in particular, they can become uniform or even bimodal.

The MD simulations presented above corroborate Boltzmann's ergodic hypothesis [49] both for the NVE and the NVE**PG** ensembles. The proofs of ergodicity for similar systems use the so-called Chernov-Sinai *Ansatz*, namely the almost sure hyperbolicity of singular orbits [50]; hyperbolicity means a non-zero Lyapunov exponent almost everywhere with respect to the Liouville measure. It was Sinai who, earlier [51], had updated Boltzmann's ergodic hypothesis. One should prove that every hard-ball system on a flat torus is fully hyperbolic

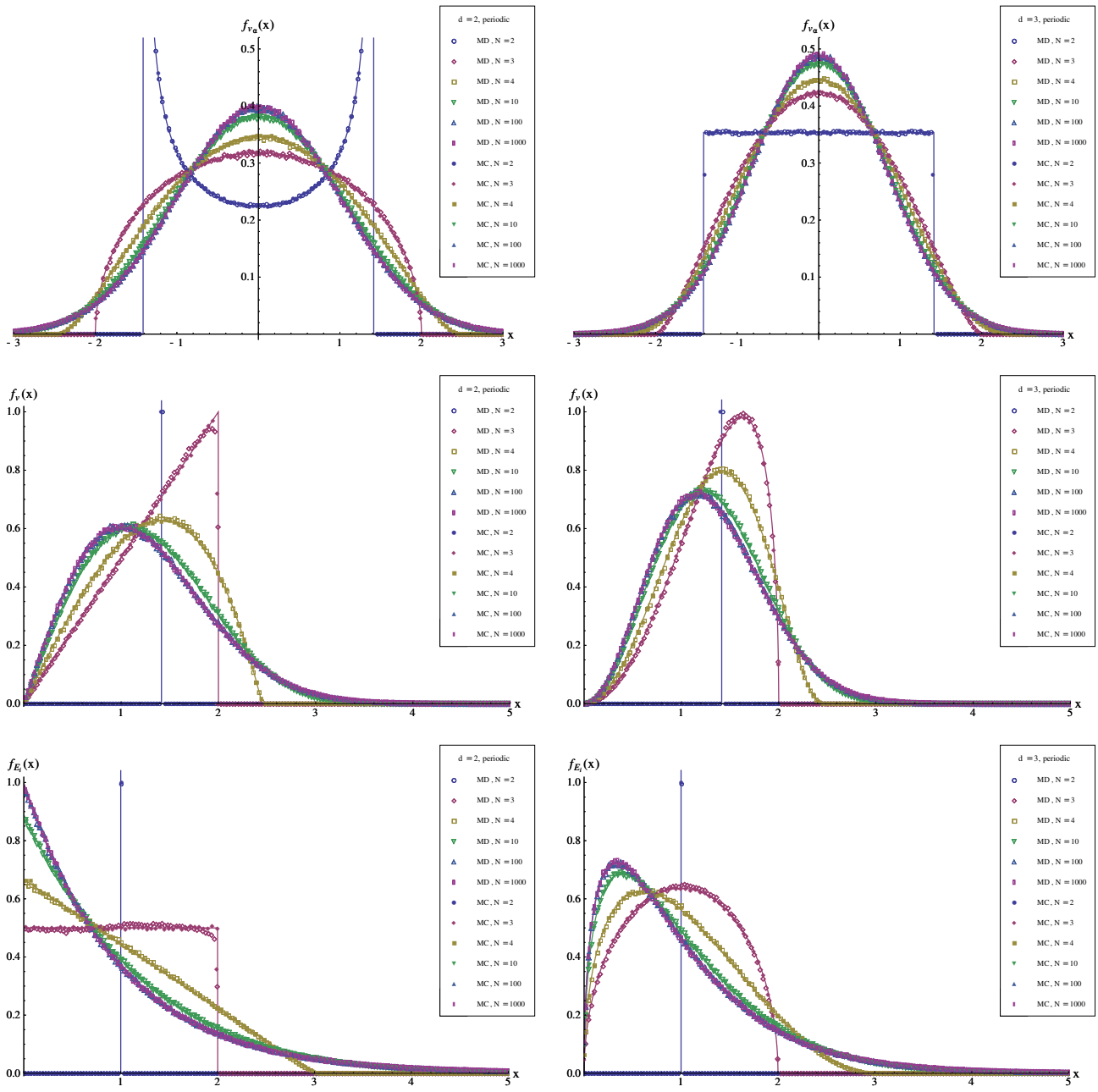

FIG. 3: (Color online) Probability density functions $f_{v_{i\alpha}}$ of the velocity components (top), f_{v_i} of the velocity modulus (middle), and f_{E_i} of the energy (bottom) for $d = 2$ (left) and $d = 3$ (right) with $\bar{E} = 1$ in the molecular dynamics ensemble (constant $NVE\mathbf{PG}$, periodic boundary conditions): theory (lines), MD (empty symbols), and MC (full symbols). Delta functions are made visible by a vertical line for the theory and by rescaling down to 1 the data point that would otherwise be out of scale.

and ergodic, after fixing its total energy, momentum, and center of mass. This rephrasing of Boltzmann's hypothesis is known as the Boltzmann-Sinai ergodic hypothesis. More recently, Simányi proved the Boltzmann-Sinai ergodic hypothesis in full generality for hard ball systems [52].

MD simulations show that Khinchin's *Ansatz* is justified for systems of hard balls. We would like to stress that this is a consequence of the microscopic dynamics and not of any a priori maximum-entropy principle. The uniform distribution on the accessible phase-space region is indeed the maximum-entropy distribution. Therefore, maximum-entropy methods do work well and all the distributions in Sec. II could be obtained by maximum-entropy methods: the beta and gamma distributions are actually the maximum-entropy distributions with given first moment, and possibly some other constraint, on a finite and a semi-infinite interval respectively. However,

this is so only because the dynamics uniformly samples the accessible phase-space region and not the other way round. In different frameworks, e.g. in biology or economics, maximum-entropy assumptions might lead to wrong results for the equilibrium distribution of a system, if its dynamics is not specified or carefully studied.

The distributions derived in Sec. II are a benchmark for random partition models popular in econophysics. Pure exchange models often lead to the same distributions [53–57].

VII. ACKNOWLEDGMENTS

We are thankful to Ubaldo Garibaldi for pointing us to the Dirichlet distribution as the multivariate generalization of the beta distribution. We are grateful to Mauro Politi for observing that the beta distribution maximizes the entropy on a finite interval given some constraints that include the first moment, even if we did not use this property in the theory exposed in Sec. II. This paper was partially supported by Italian MIUR grant PRIN 2009 2009H8WPX5 "The growth of firms and countries: distributional properties and economic determinants — Finitary and non-finitary probabilistic models in economics".

[1] J. C. Maxwell, Phil. Mag. **19**, 19 (1860).
[2] P. W. Atkins, *Physical Chemistry* (Oxford University Press, Oxford, 1978).
[3] I. Maizlish, Phys. Rev. **30**, 39 (1922).
[4] J. C. Maxwell, Phil. Trans. R. Soc. London **157**, 49 (1860).
[5] L. Desvillettes, C. Graham, and S. Méléard, Stoch. Proc. Appl. **84**, 115 (1999).
[6] C. Graham and S. Méléard, Commun. Math. Phys. **205**, 551 (1999).
[7] N. Fournier and S. Méléard, Markov Process. Related Fields **7**, 159 (2001).
[8] N. Fournier and S. Méléard, Monte Carlo Methods Appl. **7**, 177 (2001).
[9] N. Fournier and S. Méléard, J. Stat. Phys. **104**, 359 (2001).
[10] L. Boltzmann, Wien. Ber. **58**, 517 (1868).
[11] L. Boltzmann, Wien. Ber. **63**, 397 (1871).
[12] L. Boltzmann, Wien. Ber. **63**, 679 (1871).
[13] R. C. Tolman, *The Principles of Statistical Mechanics* (Oxford University Press, Oxford, 1938).
[14] D. ter Haar, *Elements of Statistical Mechanics* (Rinehart & Company, New York, 1954).
[15] L. Boltzmann, Wien. Ber. **66**, 275 (1872).
[16] J. C. Maxwell, in *Maxwell on Heat and Statistical Mechanics*, edited by E. Garber, S. G. Brush, and C. W. F. Everitt (Cambridge University Press, Cambridge, 1995), p. 123.
[17] J. Uffink, in *Stanford Encyclopedia of Philosophy*, edited by E. N. Zalta (Stanford University, Stanford, 2008), URL `http://plato.stanford.edu/entries/statphys-Boltzmann`.
[18] D. Costantini and U. Garibaldi, Stud. Hist. Phil. Mod. Phys. **28**, 483 (1997).
[19] D. Costantini and U. Garibaldi, Stud. Hist. Phil. Mod. Phys. **29**, 37 (1998).
[20] L. Brillouin, Ann. Phys. Paris **7**, 315 (1927).
[21] O. Penrose, *Foundations of Statistical Mechanics* (Pergamon Press, Oxford, 1970), hardcover ed.
[22] E. Scalas, E. Martin, and G. Germano, Phys. Rev. E **76**, 011104 (2007).
[23] U. Garibaldi and E. Scalas, *Finitary Probabilistic Methods in Econophysics* (Cambridge University Press, Cambridge, 2010).
[24] A. I. Khinchin, *Mathematical Foundations of Statistical Mechanics* (Dover, New York, 1949).
[25] D. Song and A. K. Gupta, P. Am. Math. Soc. **125**, 595 (1997).
[26] R. B. Shirts, S. R. Burt, and A. M. Johnson, J. Chem. Phys. **125**, 164102 (2006).
[27] M. J. Uline, D. W. Siderius, and D. S. Corti, J. Chem. Phys. **128**, 124301 (2008).
[28] B. J. Alder and T. E. Wainwright, J. Chem. Phys. **27**, 1208 (1957).
[29] B. J. Alder and T. E. Wainwright, J. Chem. Phys. **31**, 459 (1959).
[30] M. P. Allen and D. J. Tildesley, *Computer Simulation of Liquids* (Oxford University Press, Oxford, 1989), paperback ed.
[31] D. C. Rapaport, *The Art of Molecular Dynamics Simulation* (Cambridge University Press, Cambridge, 2004), 2nd ed.
[32] D. C. Rapaport, J. Comput. Phys. **34**, 184 (1980).
[33] N. M. Josuttis, *The C++ Standard Library — A Tutorial and Reference* (Addison-Wesley, Boston, 1999).
[34] M. Marin and P. Cordero, Comput. Phys. Commun. **92**, 214 (1995).
[35] G. Paul, J. Comput. Phys. **221**, 615 (2007).
[36] J. J. Erpenbeck and W. W. Wood, in *Statistical Mechanics B. Modern Theoretical Chemistry*, edited by B. J. Berne (Plenum Press, New York, 1977), vol. 6, pp. 1–40.
[37] B. D. Lubachevsky, J. Chem. Phys. **94**, 255 (1991).
[38] M. Marin, D. Risso, and P. Cordero, J. Comput. Phys. **109**, 306 (1993).
[39] M. Isobe, Int. J. Mod. Phys. C **10**, 1281 (1999).
[40] S. Miller and S. Luding, J. Comput. Phys. **193**, 306 (2003).
[41] H. Sigurgeirsson, *Particle field models: Algorithms and applications* (2002), Ph.D. Thesis, Scientific Computing and Computational Mathematics Program, Stanford University.
[42] S. P. Meyn and R. L. Tweedie, *Markov Chains and Stochastic Stability* (Springer, London, 1993).

[43] A. N. Kolmogorov, Giornale dell'Istituto Italiano degli Attuari **4**, 1 (1933).
[44] N. Smirnov, Recueil Mathématique (Matematiceskii Sbornik) **6 (48)**, 3 (1939).
[45] F. J. Massey, J. Am. Stat. Assoc. **46**, 68 (1951).
[46] H. W. Lilliefors, J. Am. Stat. Assoc. **62**, 399 (1967).
[47] C. M. Jarque and A. K. Bera, Econ. Lett. **6**, 255 (1980).
[48] C. M. Jarque and A. K. Bera, Econ. Lett. **7**, 313 (1981).
[49] D. Szász, Studia Sci. Math. Hung. **31**, 201 (1999).
[50] Y. Sinai and N. I. Chernov, Russ. Math. Surv. **42**, 181 (1987).
[51] Y. G. Sinai, in *Statistical Mechanics: Foundations and Applications*, edited by T. A. Bak (W. A. Benjamin, New York, 1967), pp. 559–572.
[52] N. Simányi, *The Boltzmann-Sinai ergodic hypothesis in full generality* (2010), preprint, URL `http://arxiv.org/abs/1007.1206`.
[53] M. Patriarca, A. Chakraborti, K. Kaski, and G. Germano, in *Econophysics of Wealth Distributions*, edited by A. Chatterjee, S. Yarlagadda, and B. K. Chakrabarti (Springer, Milan, 2005), pp. 93–110, arXiv:physics/0504153.
[54] M. Patriarca, A. Chakraborti, and G. Germano, Physica A **369**, 723 (2006).
[55] E. Scalas, U. Garibaldi, and S. Donadio, Eur. Phys. J. B **53**, 267 (2006).
[56] U. Garibaldi, E. Scalas, and P. Viarengo, Eur. Phys. J. B **60**, 241 (2007).
[57] D. Matthes and G. Toscani, J. Stat. Phys. **130**, 1087 (2008).